arXiv:1402.2070v1 [nucl-th] 10 Feb 2014

Softness of Sn isotopes in relativistic semi-classical approximation

S. K. Biswal, S. K. Singh, M. Bhuyan and S. K. Patra
Institute of Physics, Sachivalaya Marg, Bhubaneswar-751 005, India.
(Dated: February 11, 2014)

Within the frame-work of relativistic Thomas-Fermi and relativistic extended Thomas-Fermi approximations, we calculate the giant monopole resonance (GMR) excitation energies for Sn and related nuclei. A large number of non-linear relativistic force parameters are used in this calculations. We find that a parameter set is capable to reproduce the experimental monopole energy of Sn isotopes, when its nuclear matter compressibility lies within $210-230$ MeV, however fails to reproduce the GMR energy of other related nuclei. That means, simultaneously a parameter set can not reproduce the GMR values of Sn and other nuclei.

PACS numbers: 24.30.Cz, 21.10.Re, 24.10.Jv, 21.65.-f, 21.60.Ev, 21.65.Mn

I. INTRODUCTION

Incompressibility of nuclear matter, also knows as compressional modulus has a special interest in pure nuclear and astro-nuclear physics, because of its fundamental role in guiding the equation of state (EOS) for nuclear matter. Compressional modulus K_∞ can not be measured by any experimental technique directly, rather it depends indirectly on the experimental measurement of isoscalar giant monopole resonance (ISGMR) for its conformation [1]. This fact enriches the demand of correct measurement of excitation energy of ISGMR. The relativistic parameter with random phase approaches (RPA) constraint the range of the compressibility modulus 270 ± 10 MeV [2, 3] for nuclear matter. Similarly, the non-relativistic formalism with Hartree-Fock (HF) plus RPA allows the acceptable range of compressibility modulus $210 - 220$ MeV, which is less than relativistic one. It is believed that the part of this discrepancy in the acceptable range of compressional modulus comes from the diverse behavior of the density dependence of symmetry energy in relativistic and non-relativistic formalism [4, 5]. Now, both the relativistic and non-relativistic formalisms come with a general agreement on the value of nuclear compressibility i.e., 240 ± 10 MeV [6–8]. But the new experiment on Sn isotopic series i.e., $^{112}Sn -^{124} Sn$ rises the question "why Tin is so fluffy ?"[9–11]. This question again finger towards the correct theoretical investigation of compressibility modulus.

Thus, it is worthy to investigate the compressibility modulus in various theoretical formalisms. Most of the relativistic and non-relativistic theoretical models reproduce the strength distribution very well for medium and heavy nuclei, like ^{90}Zr and ^{208}Pb, respectively. But at the same time it overestimate the excitation energy of Sn around 1 MeV. This low value of excitation energy demands lower value nuclear matter compressibility. This gives a new challenge to both the theoretical and experimental nuclear physicsts. Till date, lots of effort have been devoted to solve this problem like inclusion of pairing effect [12–15], mutually enhancement effect (MEM) etc. [16]. But the pairing effect reduces the theoretical excitation energy only by 150 KeV in Sn isotopic series, which may not be sufficient to overcome the puzzle. Similarly, new experimental data are not in favor of MEM effect[17]. Measurement on excitation energy of $^{204,206,208}Pb$ shows that the MEM effect isotopic series.

Here, in the present work, we use the relativistic Thomas-Fermi (RTF) and relativistic extended Thomas-Fermi (RETF) [18–22] with scaling and constraint approaches in the framework of non-linear $\sigma - \omega$ model [23]. The RETF is the $\hbar^2$ correction to the RTF, where variation of density taken care properly mostly in the surface of the nucleus [24]. The RETF formalism is more towards the quantal Hartee approximation. It is also verified that the semiclassical approximation like Thomas-Fermi method is very useful in calculation of collective property of nucleus, like giant monopole resonance (GMR). In particular, for heavier mass nuclei, it gives almost similar results with the complicated quantal calculation. This is because of quantal correction are averaged out in heavier mass nuclei and results are inclined toward semiclassical one. So it is very much instructive to calculate excitation energy of various nucleus by this method and compared with experimental results. Since, last one decade, the softness of Sn isotopes remain a headache for both theorists and experimentalists, it is worthy to discuss the softness of Tin isotopes in semiclassical approximations like RETF and RTF.

Here, we calculate the excitation energy of Sn isotopes from ^{112}Sn to ^{124}Sn using the semi-classical RTF and RETF model. The different momentum ratio like $(m_3/m_1)^{1/2}$ and $(m_1/m_{-1})^{1/2}$ are compared with the scaling and constraint calculations. The theoretical results are computed in various parameter sets such as NL-SH, NL1, NL2, Nl3 and FSUG. We analyzed the predictive power of these parameter sets and discussed various aspects of the compressibility modulus.

This paper is organized as follow: In Section II we have summarized the theoretical formalisms, which are useful for the present analysis. In section III, we have given the discussions of our results. Here, we have elaborated the giant monopole resonance obtained by various parameter sets and their connectivity with compressibility modulus. The last section is devoted to a summary and concluding remarks.

II. THEORETICAL FRAMEWORK

The principle of scale invariance is used to obtain the virial theorem for the relativistic mean field [25] theory by working in the relativistic Thomas–Fermi (RTF) and relativistic

29]. Although, the scaling and constrained calculations are not new, the present technique is developed first time by Patra et al [26, 30], which is different from other scaling formalisms.

The detail formalisms of the scaling method are given in Refs. [26, 31]. For completeness, we have outlined briefly some of the essential expressions, which are needed for the present purpose. We have worked with the non-linear Lagrangian of Boguta and Bodmer [23] to include the many-body correlation arises from the non-linear terms of the $\sigma-$meson self-interaction [32–34] for nuclear many-body system. The nuclear matter compressibility modulus K_∞ also reduces dramatically by the introduction of these terms, which motivates to work with this non-liner Lagrangian. The relativistic mean field Hamiltonian for a nucleon-meson interacting system is written by [25, 26]:

$$\begin{aligned}\mathcal{H} &= \sum_i \varphi_i^\dagger \Big[-i\vec{\alpha}\cdot\vec{\nabla} + \beta m^* + g_v V + \frac{1}{2} g_\rho R \tau_3 \\ &+ \frac{1}{2} e\mathcal{A}(1+\tau_3)\Big]\varphi_i + \frac{1}{2}\left[(\vec{\nabla}\phi)^2 + m_s^2\phi^2\right] + \frac{1}{3}b\phi^3 \\ &+ \frac{1}{4}c\phi^4 - \frac{1}{2}\left[(\vec{\nabla}V)^2 + m_v^2 V^2\right] \\ &- \frac{1}{2}\left[(\vec{\nabla}R)^2 + m_\rho^2 R^2\right] - \frac{1}{2}\left(\vec{\nabla}\mathcal{A}\right)^2 - \frac{\zeta_0}{24} g_v^4 V^4 \quad (1) \\ &- \Lambda_V g_v^2 {g_\rho}^2 R^2 V^2 \quad (2)\end{aligned}$$

Here m, m_s, m_v and m_ρ are the masses for the nucleon (with $m^* = m - g_s\phi$ being the effective mass of the nucleon), $\sigma-$, $\omega-$ and $\rho-$mesons, respectively and φ is the Dirac spinor. The field for the σ-meson is denoted by ϕ, for ω-meson by V, for ρ-meson by R (τ_3 as the 3^{rd} component of the isospin) and for photon by A. g_s, g_v, g_ρ and $e^2/4\pi$=1/137 are the coupling constants for the σ, ω, ρ-mesons and photon respectively. b and c are the non-linear coupling constants for σ mesons. By using the classical variational principle we obtain the field equations for the nucleon and mesons. In semi-classical approximation, we can write the above Hamiltonian in term of density as:

$$\mathcal{H} = \mathcal{E} + g_v V\rho + g_\rho R\rho_3 + e\mathcal{A}\rho_p + \mathcal{H}_f, \quad (3)$$

where

$$\mathcal{E} = \sum_i \varphi_i^\dagger \Big[-i\vec{\alpha}\cdot\vec{\nabla} + \beta m^* \Big]\varphi_i, \quad (4)$$

$$\rho_s = \sum_i \varphi_i^\dagger \varphi, \quad (5)$$

$$\rho = \sum_i \bar{\varphi}_i \varphi, \quad (6)$$

$$\rho_3 = \frac{1}{2}\sum \varphi_i^\dagger \tau_3 \varphi_i, \quad (7)$$

and $\mathcal{H}_f$ is the free part of the Hamiltonian. The total density ρ is the sum of proton ρ_p and neutron ρ_n densities. The semi-classical ground-state meson fields are obtained by solving the Euler–Lagrange equations $\delta\mathcal{H}/\delta\rho_q = \mu_q$ ($q = n, p$).

$$(\Delta - m_s^2)\phi = -g_s\rho_s + b\phi^2 + c\phi^3, \quad (8)$$

$$\begin{aligned}(\Delta - m_v^2)V &= -g_v\rho + 2\Lambda_V R^2 V \quad (9) \\ &+ \frac{\zeta_0}{6} g_v^4 V^3 \quad (10)\end{aligned}$$

$$(\Delta - m_\rho^2)R = -g_\rho\rho_3 + 2\Lambda_V R V^2, \quad (11)$$

$$\Delta\mathcal{A} = -e\rho_p. \quad (12)$$

The above field equations are solved self-consistently in an iterative method.

$$\begin{aligned}\mathcal{H} = \mathcal{E} + \frac{1}{2}g_s\phi\rho_s^{eff} + \frac{1}{3}b\phi^3 + \frac{1}{4}c\phi^4 + \frac{1}{2}g_v V\rho + \frac{1}{2}g_\rho R\rho_3 + \frac{1}{2}e\mathcal{A}\rho_p \\ - 2\Lambda_V R^2 V^2 - \frac{\zeta_0}{12}{g_v}^4 V^4, \quad (13)\end{aligned}$$

with

$$\rho_s^{eff} = g_s\rho_s - b\phi^2 - c\phi^3. \quad (14)$$

In order to study the monopole vibration of the nucleus we have scaled the baryon density [26]. The normalized form of the baryon density is given by

$$\rho_\lambda(\mathbf{r}) = \lambda^3 \rho(\lambda r), \quad (15)$$

λ is the collective co-ordinate associated with the monopole vibration. As Fermi momentum and density are inter-related, the scaled Fermi momentum is given by

$$K_F q\lambda = \left[3\pi^2\rho_q\lambda(\mathbf{r})\right]^{\frac{1}{3}}. \quad (16)$$

Similarly ϕ, V, R and Coulomb fields are scaled due to self-consistence eqs. (7-10). But the ϕ field can not be scaled simply like the density and momentum, because the source term of ϕ field contains the ϕ field itself. In semi-classical formalism, the energy and density are scaled like

$$\begin{aligned}\mathcal{E}_\lambda(\mathbf{r}) &= \lambda^4\tilde{\mathcal{E}}(\lambda\mathbf{r}) \\ &= \lambda^4[\tilde{\mathcal{E}}_0(\lambda\mathbf{r}) + \tilde{\mathcal{E}}_{\mathbf{2}}(\lambda\mathbf{r})], \quad (17)\end{aligned}$$

$$\rho_{s\lambda}(\mathbf{r}) = \lambda^{\mathbf{3}}\tilde{\rho}_{\mathbf{s}}(\lambda\mathbf{r}). \quad (18)$$

The symbol $\sim$ shows an implicit dependence of $\tilde{m}^*$. With all these scaled variables, we can write the Hamiltonian as:

$$\begin{aligned}\mathcal{H}_\lambda &= \lambda^3\lambda\tilde{\mathcal{E}} + \frac{1}{2}g_s\phi_\lambda\tilde{\rho}_s^{eff} + \frac{1}{3}\frac{b}{\lambda^3}\phi_\lambda^3 + \frac{1}{4}\frac{c}{\lambda^3}{\phi_\lambda}^4 \\ &+ \frac{1}{2}g_v V_\lambda\rho + \frac{1}{2}g_\rho R_\lambda\rho_3 + \frac{1}{2}eA_\lambda\rho_p \quad (19) \\ &- 2\Lambda_V {R_\lambda}^2 {V_\lambda}^2 - \frac{\zeta_0}{12}g^4{V_\lambda}^4 \quad (20)\end{aligned}$$

Here we are interested to calculate the monopole excitation energy which is defined as $E^s = \sqrt{\frac{C_m}{B_m}}$ with C_m is the restoring force and B_m is the mass parameter. In our calculations, C_m is obtained from the double derivative of the scaled energy with respect to the scaled co-ordinate λ at $\lambda = 1$ and is defined as [26]:

$$C_m = \int dr \Big[-m\frac{\partial \tilde{\rho_s}}{\partial \lambda} + 3\Big({m_s}^2\phi^2 + \frac{1}{3}b\phi^3 - {m_v}^2V^2 - {m_\rho}^2R^2\Big) - (2{m_s}^2\phi + b\phi^2)\frac{\partial \phi_\lambda}{\partial \lambda} + 2{m_v}^2V\frac{\partial V_\lambda}{\partial \lambda} + 2{m_\rho}^2R\frac{\partial R_\lambda}{\partial \lambda}\Big]_{\lambda=1}, \quad (21)$$

and the mass parameter B_m of the monopole vibration can be expressed as the double derivative of the scaled energy with the collective velocity $\dot{\lambda}$ as

$$B_m = \int drU(\mathbf{r})^2\mathcal{H}, \quad (22)$$

where $U(\mathbf{r})$ is the displacement field, which can be determined from the relation between collective velocity $\dot{\lambda}$ and velocity of the moving frame,

$$U(\mathbf{r}) = \frac{\mathbf{1}}{\rho(\mathbf{r})\mathbf{r^2}}\int \mathbf{dr'}\rho_\mathbf{T}(\mathbf{r'})\mathbf{r'^2}, \quad (23)$$

with ρ_T is the transition density defined as

$$\rho_T(\mathbf{r}) = \frac{\partial \rho_\lambda(\mathbf{r})}{\partial \lambda}\Big|_{\lambda=1} = 3\rho(\mathbf{r}) + \mathbf{r}\frac{\partial \rho(\mathbf{r})}{\partial \mathbf{r}}, \quad (24)$$

taking $U(\mathbf{r}) = \mathbf{r}$. Then the mass parameter can be written as $B_m = \int drr^2\mathcal{H}$. In non-relativistic limit, ${B_m}^{nr} = \int drr^2m\rho$ and the scaled energy ${E_m}^s$ is $\sqrt{\frac{m_3}{m_1}}$. The expressions for m_3 and m_1 can be found in [35]. Along with the scaling calculation, the monopole vibration can also be studied with constrained approach [35–39]. In this method, one has to solve the constrained functional equation:

$$\int dr\left[\mathcal{H} - \eta r^2\rho\right] = E(\eta) - \eta\int drr^2\rho. \quad (25)$$

Here the constrained is $\langle R^2\rangle_0 = \langle r^2\rangle_m$. The constrained energy $E(\eta)$ can be expanded in a harmonic approximation as

$$E(\eta) = E(0) + \frac{\partial E(\eta)}{\partial \eta}|_{\eta=0} + \frac{\partial^2 E(\eta)}{\partial \eta^2}|_{\eta=0}. \quad (26)$$

The second order derivative in the expansion is related with the constrained compressibility modulus for finite nucleus K_A^c as

$${K_A}^c = \frac{1}{A}{R_0}^2\frac{\partial^2 E\eta}{\partial R_\eta}, \quad (27)$$

and the constrained energy ${E_m}^c$ as

$${E_m}^c = \sqrt{\frac{AK_A^c}{R_c}}. \quad (28)$$

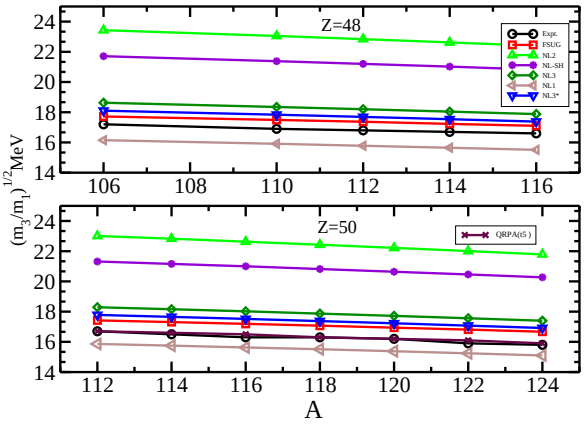

FIG. 1: Giant monopole excitation energy obtained by scaling method with various parameter sets are compared with experimental [9–11] $(m_3/m_1)^{1/2}$ for Cd and Sn isotopes.

In the non-relativistic approach, the constrained energy is related by the sum rule weighted ${E_m}^c = \sqrt{\frac{m_1}{m_{-1}}}$. Now the scaling and constrained excitation energies of the monopole vibration in terms of the non-relativistic sum rules will help us to calculate σ, i.e. the resonance width [35, 40],

$$\sigma = \sqrt{({E_m}^s)^2 - ({E_m}^c)^2} = \sqrt{(\frac{m_3}{m_1})^2 - (\frac{m_1}{m_{-1}})^2}. \quad (29)$$

III. RESULTS AND DISCUSSIONS

It is interesting to apply the model to calculate the excitation energy of Sn isotopic series and compared with experimental results. Thus, we calculate the GMR energy using both the scaling and constraint methods in the frame-work of relativistic extended Thomas-Fermi approximation using various parameter sets for Z= 48 and 50 and compared with the excitation energy with momentum ratio m_3/m_1 and m_1/m_{-1} obtained from multipule decomposition analysis (MDA). The basic reason to take a number of parameter sets is that the infinite nuclear matter compressibility of these forces cover a wide range of values. For example, NL-SH has compressibility 399 MeV, while that of NL1 is 210 MeV. From MDA analysis we get different momentum ratio, such as m_3/m_1, m_0/m_1 and m_1/m_{-1}. These ratios are connected to scaling, centroid and constraint energies, respectively. That is why we compared our theoretical scaling result with $(m_3/m_1)^{1/2}$ and $(m_1/m_{-1})^{1/2}$ with the constrained calculations.

In Figures 1 and 2 we have shown the $(m_3/m_1)^{1/2}$ and $(m_1/m_{-1})^{1/2}$ ratio for isotopic chains of Cd and Sn. The results are also compared with experimental data obtained from (RCNP) [9–11]. From the figures, it is cleared that the experimental value lies between the results obtained from FUSG (FSUGold) and NL1 force parameters. It is to be noted that, throughout the calculations, we have used only the non-linner

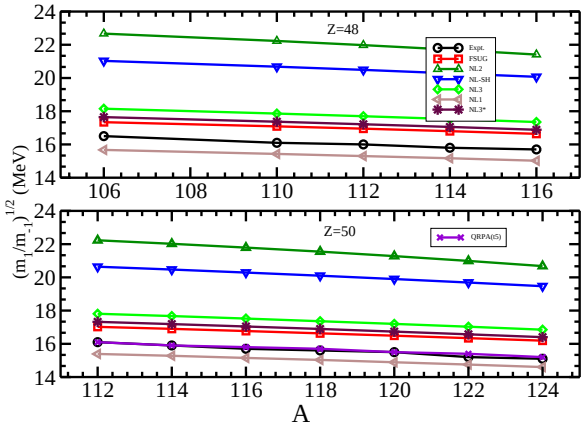

FIG. 2: Same as Fig. 1, but for $(m_1/m_{-1})^{1/2}$.

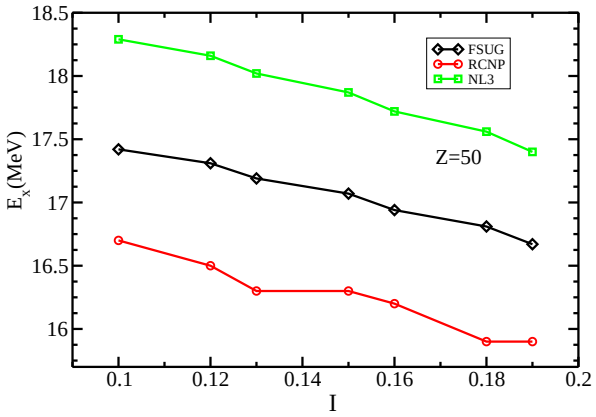

FIG. 3: The variation of giant monopole excitation energy E_X with proton-neutron asymmetry I=(N-Z)/(N+Z) for Sn isotopes.

ables with the experimental data. If one compares the experimental and theoretical results for ^{208}Pb, the FSUG set gives better results amongst all. For example, the experimental and theoretical data are 14.17$\pm$0.1 and 14.04 MeV, respectively. These values are well matched with each other. From this, one could conclude that the infinite nuclear matter compressibility lies nearer to that of FSUG (230.28 MeV) parameter. But experimental result on ISGM in RCNP shows that the predictive power of FUSG is not good enough for the excitation energy of Sn isotopes. This observation is not only confined to RCNP formalism, but also persists in the more sophisticated RPA approach. In Table I, we have given the results for QRPA(T6), RETF(FSUG) and RETF(NL1). The experimental data are also given to compare all these theoretical results.

The infinite nuclear matter compressibility K_∞ with T6 parameter set is 236 MeV and that of FSUG is 230.28 MeV. The difference in K_∞ between these two sets is only 6 MeV. The similarity in compressibility (small difference in K_∞) may be a reason for their prediction in equal value of GMR. The table shows that, there is only 0.1 MeV difference in QRPA(T5) and RETF(FSU) results in the GMR values for ^{112}Sn$-^{116}$Sn isotopes, but the results are exactly matched for the ^{118}Sn$-^{124}$Sn. This implies that for relatively higher mass nuclei, both the QRPA(T6) and RETF(FSUG) results are almost similar. If some one consider the experimental value of Sn isotopic series, then QRPA(T5) gives better result. For example, experimental value of $(m_3/m_1)^{1/2}$ for ^{112}Sn is 16.7$\pm$ 0.2 MeV and that for QRPA(T5) is 16.6 MeV. These two values matches well with each other. The infinite nuclear matter compressibility of T5 set is 202 MeV. It is shown by V. Tselyaev et al. [41] that the T5 parameter set with such compressibility, better explains the excitation energy of Sn isotopes, but fails to predict the excitation energy of ^{208}Pb. It over estimates the data for ^{208}Pb. The experimental data of ISGMR energies for ^{90}Zr and ^{114}Sn lies in between the calculated values of T5 and T6 forces. In summary, we can say that the RPA analysis predicts the symmetric nuclear matter

calculation gives it in the range $210-230$ MeV. These two predictions almost agree with each other in the acceptable limit.

In Table II, we have displayed the data obtained from a recent experiment [17] and compared our results. Column two of the table is also devoted to the result obtained from pairing plus MEM effect [15]. The data show clearly that our result (extended Thomas-Fermi) has a priority over the pairing + MEM prediction. For example, the difference between the pairing+MEM results and experimental observation is 0.3 MeV for ^{204}Pb isotopes, which is away from the experimental error, while it is only 0.1 MeV (within the error bar) in the RETF and data. This trend also followed by ^{206}Pb and ^{208}Pb nuclei. In our model, we have not included any pairing externally. But still our results are good enough in comparision with MEM+pairing. This implies two things: (i) pairing may not be impotant in calculation of excitation energy or (ii) pairing effect is automatically included in Thomas-Fermi calculations. To our understanding, the second option seems to be more appropiate, because lots of work show that pairing must be included for the calculation of excitation energy of open shell nuclei. Fig. 3 shows the variation of excitation energy with proton-neutron asymetry in Sn isotopes. Here, we want to know, how the excitation energy varies with asymetry or more specifically, "is the variation of experimental excitation energy with asymetry same that of theoritical one ?". The graph shows that the variation with both NL1 and FSUG are following similar partten as experimental one with a different mangnitued as shown in the figure.

In Figure 4, we have compared the results obtained from RETF and RTF with the experimental data for Sn isotopes. The celebraty NL3 parameter set is used in the calculations. The graph shows that there is only a small difference ($\sim$ 0.2 MeV) in RETF and RTF results. Interestingly, the RETF correction is additive to the RTF result instead of softening the excitation energy of Sn isotopes. Then the natural question arises: is it the brhavior for all the parameter sets in RETF approximation ?. To attend the question, we plotted Fig. 5, where we have shown the difference of $\sqrt{m_3/m_1}$ obtained

TABLE I: Momentum ratio for Sn isotopes using RETF approximation with FSUGold and NL1 sets are compared with QRPA(T6) predictions [41].

Nucleus	$(m_3/m_1)^{1/2}$(MeV)				$(m_1/m_{-1})^{1/2}$(MeV)			
	QRPA(T6)	RETF(FSUG)	RETF(NL1)	Expt.	QRPA(T6)	RETF(FSU)	RETF(NL1)	Expt.
^{112}Sn	17.3	17.42	15.86	16.7	17.0	17.2	15.39	16.1
^{114}Sn	17.2	17.32	15.75	16.5	16.9	16.9	15.28	15.9
^{116}Sn	17.1	17.19	15.63	16.3	16.8	16.77	15.15	15.7
^{118}Sn	17.0	17.07	15.51	16.3	16.6	16.63	15.03	15.6
^{120}Sn	16.9	16.94	15.38	16.2	16.5	16.44	14.89	15.5
^{122}Sn	16.8	16.81	15.24	15.9	16.4	16.34	14.75	15.2
^{124}Sn	16.7	16.67	15.1	15.8	16.2	16.19	14.6	15.1

TABLE II: Momentum ratio $\sqrt{m_1/m_{-1}}$ for Pb isotopes within RETF is compared with pairing+ MEM results and experimental data [17].

Nuclear Mass	${m_1/m_{-1}}^{1/2}$ (MeV)			Γ	
	pairing+MEM	Our work	Expt.	our work	Expt.
^{204}Pb	13.4	13.6	13.7±0.1	2.02	3.3±0.2
^{206}Pb	13.4	13.51	13.6±0.1	2.03	2.8±0.2
^{208}Pb	13.4	13.44	13.5±0.1	2.03	3.3±0.2

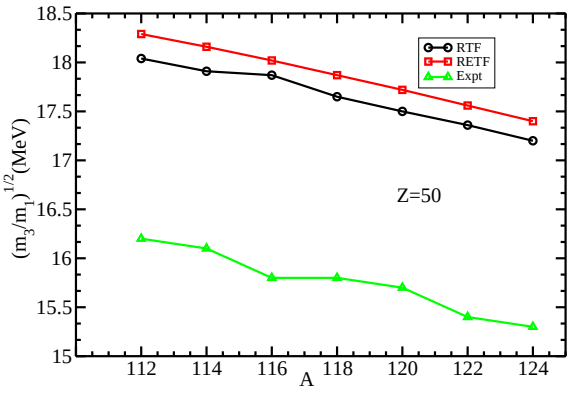

FIG. 4: The scaling monopole excitation energy within RETF and RTF formalisms compared with the experimental momentum ratio ${m_3/m_1}^{1/2}$ [17].

ter sets. For all sets, except NL1, we find RETF-RTF as positive. Thus, it is a challenging task to antangle the term which is the responsible factor to determine the sign of RETF-RTF. Surprisingly, for most of the parameter sets, RTF is more towards experimental data. Inspite of this, one cannot says anything about the qualitative behavior of RETF. Because, the variation of the density at the surface taken care properly by RETF formalism, which is essential. One more interesting observation is that, when one investigate the variation of RETF-RTF in the isotopic chain of Sn, it remains almost constant for all the parameter sets, except FSUG. In this context, FSUG behaves differently.

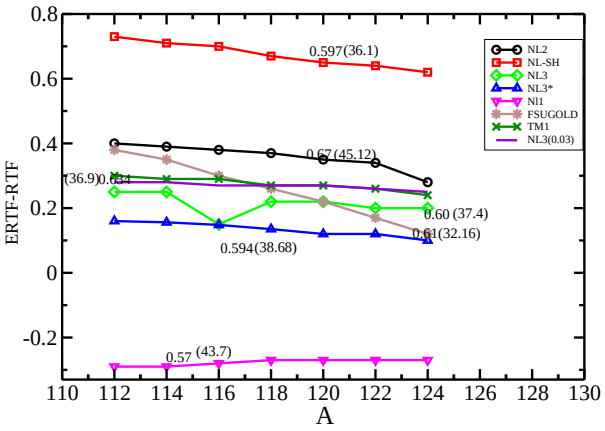

FIG. 5: The variation of the difference of giant monopole excitation energy obtained from RETF and RTF (RETF-RTF) formalisms with various parameter sets for Sn isotopic chain.

FSUG set shows that, there may be some correlation of RETF with the symmetry energy. This is clearly absent in all other parameter sets. Now it is essential to know, in which respect the FSUG parameter set is different from other. The one-to-one interaction terms for NL3, NL2, NL1 and NL-SH all have similar couplings. However, the FSUG is different from the above parameters in two aspect, i.e., two new coupling constants are added. One corresponds to the self-interaction of ω and other one corresponds to the isoscalar-isovector meson coupling. It is known that self-interaction of ω is responsible for softening the EOS [42–44] and the isoscalar-isovector coupling takes care of the softening for symmetry energy of symmetric nuclear matter[4]. The unique behavior shown by the FSUG parametrization may be due to the following three reasons:

1. introduction of isoscalar-isovector meson coupling Λ_V.
2. introduction of self-coupling of $\omega-$meson.
3. Or simultaneous introduction of both these two terms with refitting of parameter set with new constraint.

In order to discuss the first possibility, we plotted

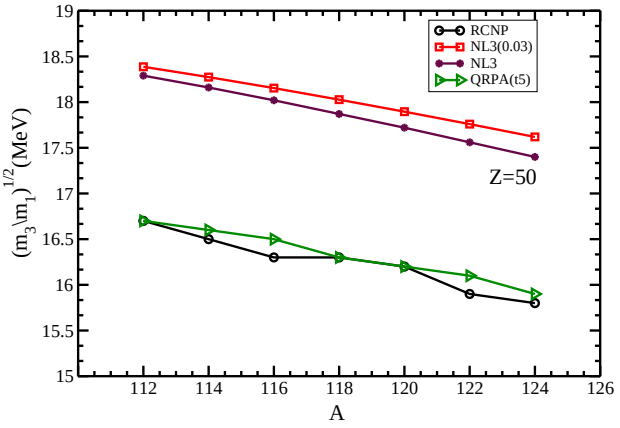

FIG. 6: The momentum ratio $\sqrt{m_3/m_1}$ for Sn isotopes obtained with NL3+Λ_V is compared with NL3, QRPA(T5) and experimental data.

no difference between NL3 and NL3+Λ, except the later set predicts a more possitive RETF-RTF. It is well known that, the addition of Λ_V coupling, i.e., NL3+Λ_V(0.03) gives of a softer symmetry energy [45]. This implies that, models with softer energy have greater difference in RETF and RTF. At a particular proton-neutron asymmetry, RETF-RTF has a larger value for a model with softer symmetry energy. This observation is not conclusive, because all the parameter sets do not follow this type of behavior. Quantitatively, the change of RETF-RTF in the Sn isotopic series is about 70%, while this is only $20-30\%$ in NL3 and other parameter set.

In Table III, we have listed the $\rho-$meson contribution to the total energy. From the analysis of our results, we find that only $\rho-$contribution to the total binding energy change much more than other quantity, when one goes from RTF to RETF. But this change is more prominent in FSUG parameter set than other sets like NL1, NL2, NL3 and NL-SH. Simple assumption says that, may be the absent of Λ_V term in other parameter is the reason behind this. But we have checked for the parameter NL3+Λ_V, which does not follow. This also shows similar behavior like other sets. In Table IV, we have given the results for FSUG, NL3+Λ_V and NL1. The data show clearly that, there is a huge difference of monopole excitation energy in RETF and RTF with FSUG parameter set. For example, the $\rho-$meson contribution to the GMR in RETF for ^{112}Sn is 21.85 MeV, while in RTF it is only 0.00467 MeV. However, this difference is nominal in NL3+Λ_V parameter set, i.e., it is only 0.48 MeV. Similarly, this value is 1.18 MeV in NL1 set. The contribution of $\rho-$meson to total energy comes from two terms: (i) one from $\Lambda_V R^2V^2$ and other (ii) from ρ^2. We have explicitly shown that contribution comes from $\Lambda_V R^2V^2$ makes a huge difference between the GMR obtained from RETF and RTF formalisms. This type of contribution does not appear from NL3+Λ_V. For example, in ^{112}Sn the contribution of $\Lambda_V R^2V^2$ with RETF formalism is -6.0878 MeV, while with RTF formalism is -5.055 MeV.

TABLE III: Contribution of the $\rho-$meson to the total binding energy in the RTF and RETF approximations with FSUGold and NL1 parameter set.

Mass	FSUG				NL3(0.03)		NL1	
	RETF	RTF	RETFΛ_V	RTFΛ_V	RETF	RTF	RETF	RTF
112	21.85	-6.66	-0.00130	0.00467	20.60	20.12	17.91	16.73
114	28.72	-8.64	-0.00202	0.00664	27.11	26.48	23.51	22.00
116	36.42	-10.83	-0.00248	0.00829	34.40	33.62	29.73	27.90
118	44.87	-13.23	-0.00298	0.01013	42.42	41.499	36.52	34.37
120	54.04	-15.82	-0.00353	0.01213	51.13	50.05	43.84	41.37
122	63.88	-18.58	-0.00411	0.01429	60.48	59.24	51.63	48.85
124	74.33	-21.49	-0.00473	0.01660	70.43	69.03	59.84	56.76

TABLE IV: ^SK_A and ^CK_A are compressibility of finite nuclei obtained from scaling and costraint methods, respectively are compared with the values obtained from the equation of state (EOS).

Nuclear Mass	NL3			FSUGOLD		
	^SK	^Ck	^{EOS}K	^SK	^CK	^{EOS}K
^{208}Pb	164.11	149.96	145	147.37	134.57	138.42
^{116}Sn	164.64	155.39	131.57	147.11	139.71	127.64
^{40}P	136.70	110.43	105	123.40	100.36	102.53
^{40}Ca	145.32	134.47	105	130.93	123.15	102.53

the contribution of Λ_V may be responsible for this anomalous behavior. But an immediate question arises , why NL3+Λ_V parameter set does not show such type of effects, inspite of having $\Lambda_V R^2V^2$ term. This may be due to the procedure in which $\Lambda_V R^2V^2$ term is added in two parameters. In NL3+Λ_V(0.03), the $\Lambda_V R^2V^2$ term is not added independently. The Λ_V and g_ρ are interdependent to each other to fix the binding energy BE and difference in neutron and proton rms radii R_n-R_p. But in FSUGold, Λ_V coupling constant is added independenly to reproduce the nuclear observables. In Table IV, we have listed the compressibility of some of the selected nuclei in scaling ^SK_A and constraint ^CK_A icalculations. This results are compared with the computed values obtained from EOS model. To evaluate the compressibility from EOS, we have followed the procedure discussed in [46, 47]. M. Centelles et al [46], parameterised the density for finite nucleus as $\rho_A = \rho_0 - \rho_0/(1 + c * A^{1/3})$ and obtained the asymmetry coefficient a_{sym} of the nucleus with mass A from the EOS at this particular density. Here also, we have used the same parametric from of the density and obtained the compressibility of finite nucleus from the EOS. For example, $\rho_A = 0.099$ for $A = 208$ in FSUG parameter set. We have calculated the compressibility from the EOS at this particular density, which comes around 145 MeV. We have also calculated the compressibility independently in Thomas-Fermi and extended Thomas-Fermi using scaling and constraint calculations, which are 161 MeV and 146.1 MeV, respectively.

IV. SUMMARY AND CONCLUSION

In summary, we analysed the predictive power of various

the frame-work of relativistic Thomas-Fermi and relativistic extended Thomas-Fermi approaches for giant monopole excitation energy of Sn-isotopes. The calculation is then extended to some other relevant nuclei. The analysis shows that Thomas-Fermi approximation gives better resluts than pairing+MEM data. It exactly reproduces the experimental data for Sn isotopes, when the compressibility of the force parameter is within $210-230$ MeV. We also concluded that a parameter set can reproduce the excitation energy of Sn isotopes, if its infinite nuclear matter compressibility lies within $210-230$ MeV, however, fails to reproduce the GMR data for other nuclei within the same accuracy.

We have qualitatively analized the difference in GMR energies RETF-RTF using RETF and RTF formalisms in various force parameters. The FSUGold parameter set shows different behavior from all other forces. Also, extended our calculations of monopole excitation energy for Sn isotopes with a force parametrization having softer symmetry energy (NL3+ Λ_V). The excitation energy decreses with the increse of proton-neutron asymetry agreeing with the experimental trend. In conclusion, after all these thorough analysis, it seems that the softening of Sn isotopes is an open problem for nuclear theory and more work in this direction are needed.

[1] J. P. Blaizot, Phys. Rep. **64**, 171 (1980).
[2] G. A. Lalazissis, J. König and P. Ring, Phys. Rev. C **55**,540 (1997).
[3] D. Vretenar, A. Wandelf and P. Ring, Phys. Lett. B **487**, 334 (2002).
[4] C. J. Horowitz and J. Piekarewicz, Phys. Rev. Lett. **86**, 5647 (2001).
[5] C. J. Horowitcz and J. Piekarewicz, Phys. Rev. C **64**, 062802 (R) (2001).
[6] G. Colo et al., Nucl. Phys. Rev. C **70**, 024307 (2004).
[7] B. G. Todd-Rutel and J. Piekarewicz, Phys. Rev. Lett. **95**, 122501 (2005).
[8] B. K. Agrawal, S. Shlomo and V. Kim Au, Phys. Rev. C **86**, 031304 (2005).
[9] U. Garg, arxiv: 1101.3125
[10] T. li et al., Phys Rev. Lett. **99**, 162503 (2007).
[11] U. Garg et al., Nucl. Phys. A **788**, 36c (2007).
[12] O. Citaverese et al., Phys. Rev. C **43**, 2622 (1991).
[13] Li-Gang Cao, H. Sagawa and G. Colo, Phys. Rev. C **86**, 054313 (2012).
[14] Jun Li et al., Phys. Rev. C **78**, 064304 (2008).
[15] E. Khan, Phys. Rev. C **80**, 011307(R) (2009).
[16] E. Khan, Phys. Rev. C **80**, 057302 (2009).
[17] D. Patel et al, arXiv:1307.4487v2 [nucl-ex].
[18] M. Centelles, X. Viña, M. Barranco and P. Schuck, Ann. Phys., NY **221**, 165 (1993).
[19] M. Centelles, X. Viñas, M. Barranco, S. Marcos and R. J. Lombard, Nucl. Phys. A **537**, 486 (1992).
[20] C. Speicher, E. Engel and R.M Dreizler, Nucl. Phys. A **562**, 569 (1993).
[21] M. Centelles, M. Del Estal and X. Viñas, Nucl. Phys. A **635**, 193 (1998).
[22] M. Centelles et al, Phys. Rev. C **47**, 1091 (1993).
[23] J. Boguta and A. R. Bodmer, Nucl. Phys. A **292**, 413 (1977).
[24] M. Centelles, X. Viñas, M. Barranco and P. Schuck, Nucl. Phys. A **519**, 73c (1990).
[25] B. D. Serot and J.D. Walecka, Adv. Nucl. Phys. **16**, 1 (1986).
[26] S. K. Patra, X. Viñas, M. Centelles and M. Del Estal, Nucl. Phys. A **703**, 240 (2002); ibid Phys. Lett. B **523**, 67 (2001); Chaoyuan Zhu and Xi-Jun Qiu, J. Phys. G **17**, L11 (1991).
[27] C. Speichers, E. Engle and R. M. Dreizler, Nucl. Phys. A **562**, 569 (1998).
[28] M. Centeless, M. Del Estal and X. Viñas, Nucl. Phys. A **635**, 193 (1998).
[29] M. Centelles, X. Viñas, M. Barranco, N. Ohtsuka, A. Faessler, Dao T. Khoa and H. Müther, Phys. Rev. C **47**, 1091 (1993).
[30] M. Centelles, S. K. Patra, X Roca-Maza, B. K. Sharma, P. D. Stevenson and X. Viñas, J. Phys. G: **37**, 075107 (2010).
[31] S. K. Patra, M. Centelles, X. Viñas and M. Del Estal, Phys. Rev. C **65**, 044304 (2002).
[32] L. I. Schiff, Phys. Rev. **80**, 137 (1950); **83**, 239 (1951); **84**, 1 (1950).
[33] Jun-ichi Fujita and Hironari Miyazawa, Prog. Theor. Phys. **17** 360 (1957).
[34] Steven C. Pieper, V. R. Pandharipande, R. B. Wiringa and J. Carlson, Phys. Rev. C **64** 014001 (2001).
[35] O. Bohigas, A. Lane and J. Martorell, Phys. Rep. **51**, 267 (1979).
[36] T. Maruyama and T. Suzuki, Phys. Lett. B **219**, 43 (1989).
[37] H. F. Boersma, R. Malfliet and O. Scholten, Phys. Lett. B **269**, 1 (1991).
[38] M. V. Stoitov, P. Ring and M. M. Sharma, Phys. Rev. C **50**, 1445 (1994).
[39] M. V. Stoitsov, M. L. Cescato, P. Ring and M. M. Sharma, J. Phys. G: **20**, L49 (1994).
[40] M. Centelles, X. Viñas, S. K. Patra, J. N. De and Tapas Sil, Phys. Rev. C **72**, 014304 (2005).
[41] V. Tselayaev, J. Speth, S. Krewald, E. Livinova, S. Kamerdzhiev, and N. Lyutorovich, Phy. Rev. C **79**, 034309 (2009).
[42] S. Gmuca, Z. Phys. A 342, 387 (1992); Nucl. Phys. A 547, 447 (1992).
[43] Y. Sugahara, H. Toki, Nucl. Phys. A **579**, 557 (1994).
[44] A. R. Bodmer, Nucl. Phys. A **157** 625 (1991)
[45] M. Centelles, S. K. Patra, X. Roca-Maza, P. D. Stevenson and X. Viñas, J. Phys. G: **37** 075107 (2009).
[46] M. Centelles, X. Roca-Maza, X. Viñas and M. Warda, Phys. Rev. Lett. **102**, 122502 (2009).
[47] S. K. Singh, M. Bhuyan, P. K. Panda and S. K. Patra, J. Phys. G: **40** 085104 (2013).